PART IV
CYCLIC VOLTAMMETRIC STUDIES

Vinod P Raphael "Physicochemical, corrosion inhibition and biological studies on schiff bases derived from heterocyclic carbonyl compounds and their metal complexes" Thesis. Department of Chemistry, St. Thomas College Thrissur, University of Calicut, 2014

PART IV

CYCLIC VOLTAMMETRIC STUDIES

CHAPTER 1

INTRODUCTION AND REVIEW

Cyclic voltammetry (CV) is an important electrochemical technique by which the redox behaviour of molecules can be determined. The rate of oxidation/reduction and the mechanism of probe coupled chemical reaction can be well established using CV studies. Redox behaviour of the chemical species helps the analyst to perform qualitative and quantitative analysis. CV analysis is accomplished with a three electrode arrangement whereby the potential relative to some reference electrode is scanned at a working electrode, while the resulting current flowing through a counter (or auxiliary) electrode is monitored in a quiescent solution. This technique is ideally suited for a quick search of redox couples present in a system. Discouraging of CV for widespread quantitative analysis is due to two important difficulties a) changing current at high scan rates and b) data analysis from the asymmetric shaped peaks.

In CV experiment (which is a simple extension of linear sweep technique), the potential of a small stationary electrode is altered linearly with time. Potential gradually changes from a region where no electrode reaction occurs, to potentials where oxidation or reduction of an analyte occurs. The direction of sweep is reversed after travelling the potential regime in which one or more electrode reaction occurs and the electrode reactions are monitored for the products or intermediates which are formed during the forward scan [1-3]. The total potential traversed and the sweep rate of the analysis determine the time of the experiment.

Similar to the polarographic analysis, the major form of mass transport is the diffusion of analyte to the electrode surface in a quiescent solution. CV is characterized by several parameters such as cathodic (E_{pc}) and anodic (E_{pa}) peak potentials, the cathodic (i_{pc}) and anodic (i_{pa}) peak currents, the cathodic half peak potential ($E_{p/2}$) and half wave potential ($E_{1/2}$). The definition of $E_{1/2}$ has been adopted from the conventional polarography, according to equation 1.

$$E_{\frac{1}{2}} = E^0 + \frac{RT}{nF} ln\left[D_{R/}D_O\right]^{1/2} \quad (1)$$

where E_0 is the formal potential pertaining to the ionic strength of the solution used, D_0 and D_R are the diffusion coefficients of the oxidized and reduced states and n is the number of electrons in the half reaction. Since $D_0 \approx D_R$, $E_{1/2}=E_0$ usually within a few mV of E_0.

Cyclic voltammetric systems can be divided into three major divisions, based on the behaviour of analyte towards the applied potential. These are a) reversible system b) irreversible system and c) quasi reversible system.

Cyclic Voltammetry of a Reversible System

When the electrode kinetics is much faster than the rate of diffusion, the system is said to be reversible. Figure 4.1 illustrates the cyclic voltammogram of are reversible system. In such systems, the electron transfer reaction at the electrode surface is so rapid that equilibrium conditions are maintained even with substantial net current and a rapidly changing potential. By the analysis of this figure, the equation for the peak current in the linear sweep voltammetry at 298K can be verified by Randles and Sevick equation (eqn 2) [4,5].

$$i_p = (2.69 \times 10^5) n^{3/2} A D_0^{1/2} C_0 v^{1/2} \quad (2)$$

where A is the area of the electrode in cm^2, D_0 is the diffusion coefficient in cm^2s^{-1}, C_0 is the concentration of the analyte in mol/cm^3, υ is the scan rate in mV/s and i_p is the peak current in amperes. For reversible systems, the peak potential E_p is given by the equation 3.

$$E_P = E^0 - 1.109\ \frac{RT}{nF} \quad (3)$$

The peak potential may be difficult to analyze, as the peak is broad and therefore it is easy to calculate the half peak potential $E_{1/2}$ at $i_{p/2}$, which is given by equation 4.

$$E_{1/2} = E^0 + 1.09\ \frac{RT}{nF} \quad (4)$$

From equation 3 and 4,

$$\left|E_P - E_{p/2}\right| = 2.20\ \frac{RT}{nF} = \frac{56.5}{n}\ mV \quad (5)$$

Equation 5 can be regarded as the first criterion for the reversibility. The separation of peak potentials i.e., E_{pa}-E_{pc} is another significant parameter in CV which can be used to ascertain the reversibility of a process.

$$\Delta E_p = E_{pa} - E_{pc} = 2.218\frac{RT}{nF} \approx \frac{57}{n}\ mV \quad (6)$$

Thus value of peak potential separation (ΔE_p) at 298K and $|E_{p/2}$-$E_{pc}|$ are independent of scan rate and concentration. The ratio of peak currents i_{pa}/i_{pc} is independent of the scan rate for reversible systems, and this is regarded as the third significant parameter.

Cyclic Voltammetry of Irreversible Systems

When the electrode kinetics is slower than the rate of diffusion, the system is said to be irreversible. For one electron, one–step irreversible process

(Ox+e→Red), inverse peak will not emerge in the cyclic voltammogram on changing the direction of scan.

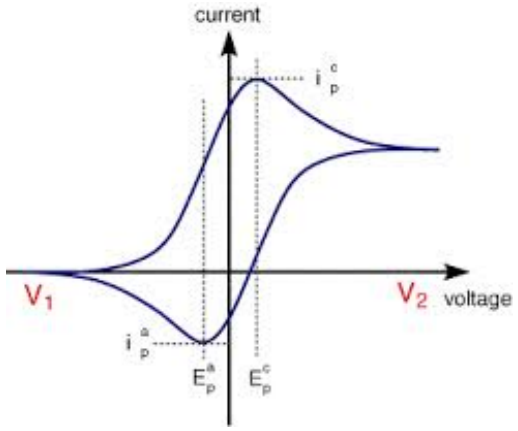

Fig. 4.1 Cyclic voltammogram of a reversible system

Since irreversible reactions give relatively very small current function (about 50%) compared to that of reversible process, a bigger overpotential is required to lead the reduction and therefore peak potential appears at higher values beyond E_0. The peak current and the peak potential for irreversible system at 298K is given by equations 7 and 8 respectively.

$$i_p = (2.99 \times 10^5)\alpha^{1/2} A D_0^{1/2} C_0 v^{1/2} \quad (7)$$

$$E_p = E^0 - \frac{RT}{\alpha F}\left[0.78 + [D_0^{1/2}/k_0]\right] + \ln\left[\frac{\alpha F v}{RT}\right]^{1/2} \quad (8)$$

From the above equations,

$$\left|E_P - E_{p/2}\right| = 2.20\ \frac{RT}{\alpha F} \quad (9)$$

where k_0 is the standard rate constant and α is the transfer coefficient. From equation 8, it is clear that for a totally irreversible system ($k_f >> k_b$ for the cathodic peak and $k_b >> k_f$ for the anodic peak), E_p depends on the scan rate [6,7]. Irreversibility manifests through ΔE_p i.e., E_{pa}-E_{pc}>(57/n) mV and ΔE_p increases

with increasing scan rate. Figure 4.2 represents the cyclic voltammogram of an electrically irreversible system.

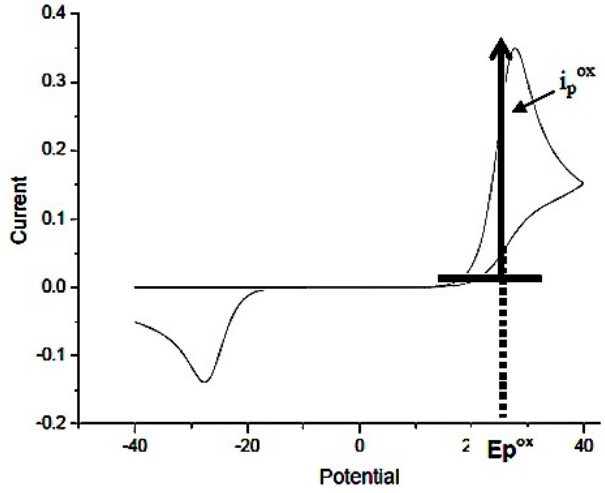

Fig. 4.2 Cyclic voltammogram of an irreversible system

Cyclic Voltammetry of Quasi-reversible Systems

Quasi-reversible systems are intermediate between reversible and irreversible systems. For such systems i_p is not sufficiently proportional to $\upsilon^{1/2}$. The peak potential is represented by an integral equation which is solved by numerical methods. For quasi reversible system, (with $10^{-1}>k_0>10^{-5}$cm/s), the current is controlled by both the charge transfer and mass transport. The shape of cyclic voltammogram is a function the ratio $\frac{k_0}{[D_0^{\frac{1}{2}}\ (F/RT)^{1/2}\upsilon^{1/2}]}$.

As the ratio increases, the process approaches to the reversible case [8,9]. The voltammogram of a quasi reversible system are more drawn out and exhibit larger separation in peak potential compared to reversible system. To calculate the rate constant for a quasi-reversible reaction (ΔE_p up to 200mV), following equation can be used.

$$\psi = k_s \frac{[\frac{D_o}{D_R}]^{\alpha/2}}{[D_0 \pi (\frac{nF}{RT})]^{1/2}} \qquad (10)$$

where ψ is a function of quasi reversible system whose values bring by numerical approach. Figure 4.3 depicts the cyclic voltammogram of a quasi reversible system.

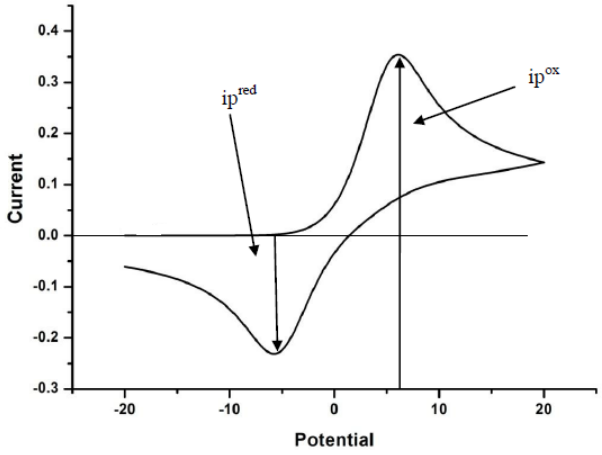

Fig. 4.3 Cyclic voltammogram of a quasi reversible system

Cyclic Voltammetric Studies on Semicarbazones and Thiosemicarbazones and Their Metal Complexes- A Review

Many organic molecules [10-15] and their metal complexes have been screened for cyclic voltammetric studies to understand the electrochemical response of the molecules. Subsequent paragraphs illustrate the summary of CV investigations on various organic molecules and complexes reported by previous researchers.

B. Lotf et al [16] have reported the anodic oxidation of 4-methoxybenzaldehyde semicarbazone derivatives examined in acetonitrile containing lithium perchlorate ($LiClO_4$) as a supporting electrolyte (20g/l). The electrode system contained a carbon paste working electrode, a platinum wire as

counter electrode and saturated calomel as reference electrode. The voltammetric curve obtained for the oxidation of 4-methoxybenzaldehyde semicarbazone shows two oxidation peak potential at 0.9V and the second at 1.35V and no reduction peak potential.

Reduction behaviour of 2-acetylpyridine semicarbazone was studied on glassy carbon electrode in CH_3OH-Britton Robinson buffer at pH 5, 7 & 9 using cyclic voltammetry by R. Sangtyani et al [17]. Single irreversible reduction wave is observed due to the reduction of semicarbazone moiety. The effect of change in pH and sweep rate was evaluated. The electrode process was found to be irreversible and diffusion controlled. Kinetic parameters were calculated from cyclic voltammetric measurements.

The electrochemical behaviour of isatin-3-hydrazone, 7-methylisatin-3-hydrazone, isatin-3-semicarbazone, isatin-3-thiosemicarbazone, 5-bromoisatin-3-thiosemicarbazone and 5-nitroisatin, at a glassy carbon electrode, using cyclic voltammetry over a wide pH range, was investigated and compared with isatin by B. S. C. Oliveirra et al [18]. Two consecutive irreversible peaks were observed by isatin-semicarbazone. Two reversible cathodic peaks were observed on the first negative going reversible cycle and peak potential separation suggests that two electron process is involved.

Recently, R. K Christian et al [19], studied the electrochemical properties of alpha-N-heterocyclic chalcogen semicarbazones (HL), namely, thiosemicarbazones, selenosemicarbazones, and semicarbazones, and their Ga(III), Fe(III), and Ru(III) complexes $[ML_2][Y]$ (M = Ga, Fe or Ru; Y = PF_6,

NO_3^- or $FeCl_4^-$) by cyclic voltammetric technique. The cyclic voltammogram of the Ga complexes displayed at least two consecutive reversible one-electron reduction waves. These reductions are shifted by approx. 0.6 V to lower potentials in the corresponding Fe and Ru complexes. The electrochemical, chemical and spectroscopic data indicate that the ligand centered reduction takes place at the C=N double bond.

A new bimetallic copper(II) complex has been synthesized with ligand, obtained by the condensation of salicylaldehyde and the amine derived from reduction of nitration product of benzyl by B. Sarma et al [20]. Cyclic voltammetry of Cu(II)L·$2H_2O$ in CH_3CN was determined using platinum disc as working electrode and Ag–AgCl electrode as the reference. The cyclic voltammetric profile was of quasi reversible one with the redox potential value +0.105 V ±0.005 V. This redox potential is due to Cu(II)/Cu(I) redox couple. The ratio of cathodic to anodic current was found to be 0.949.

S. Datta et al [21] demonstrated that reaction of salicylaldehyde semicarbazone (L^1), 2-hydroxyacetophenone semicarbazone (L^2), and 2-hydroxynaphthaldehyde semicarbazone (L^3) with $[Pd(PPh_3)_2Cl_2]$ in ethanol in the presence of a base (NEt_3) affords a family of yellow complexes. In these complexes, the semicarbazone ligands are coordinated to palladium in a rather unusual tridentate ONN-mode, and a PPh_3 also remains coordinated to the metal centre. Cyclic voltammetry on all the complexes showed an irreversible oxidation of the coordinated semicarbazone within 0.86–0.93V vs SCE, and an irreversible reduction of the same ligand within −0.96 to −1.14 V vs SCE.

The coordination behaviour of ferrocenylthiosemicarbazone was investigated in a trinuclear [Ni(Fctsc)$_2$] complex by R. Prabhakaran et al [22]. The redox behaviour of the trinuclear complex in DMF has been studied using cyclic voltammetry at 100 mV scan rate by using a platinum wire counter electrode and a platinum disc working electrode. All the potentials are referenced to Ag/AgCl electrode. The complex exhibits a pair of redox waves on both the positive and the negative potential. They confirmed that the first reduction is due to a single electron Ni(II)–Ni(I) reduction, whereas the second step, which is double in intensity, compared to the first, may be due to the concomitant reduction of both ferrocenyl subunits in two one-electron reductions. The first reduction is observed at -0.35 V for Ni(II)–Ni(I) and the second reduction is at -1.4 V corresponding to Fe(II)–Fe(I). Reversible oxidation potentials are observed for Ni(II)–Ni(III) and Fe(II)–Fe(III) at 0.2 V and 0.8 V, respectively.

Scope and Objectives of the Present Investigation

The electrochemical behaviour of many organic molecules and metal complexes has been investigated by various researchers by voltammetric studies. Majority of the investigations which are primarily done in the area of organic and inorganic fields of research, were helpful to supplement the structural features of the molecules and check the affinity of the metal ion to organic molecules which are acting as ligands. By investigating the electrochemical response of newly synthesized compounds, the probable regions in the molecule which are susceptible to oxidation or reduction process can be evaluated. This idea will be beneficial when the molecules are serving as agents especially in the electrical and

analytical fields of applications. In the present course of investigation the newly synthesized Schiff bases and their complexes were screened for their electrochemical response using cyclic voltammetry. By evaluating the voltammetric parameters, an attempt was made to categorize the molecular systems as irreversible or quasi irreversible. To check the factors which govern the rate determining step, adsorption of the molecules on the electrode surface, response towards the higher scan rates etc were the other fields of interest. An attempt was also done to propose the mechanism for the electrochemical behaviour of the synthesized molecules in DMSO.

CHAPTER 2

MATERIALS AND METHODS

The electrochemical behaviour of the Schiff bases and their complexes was investigated by cyclic voltammetric experiments. The medium of investigation was anhydrous DMSO. For performing the experiment, three electrode cell assembly was used in which platinum loop acted as the inert electrode, Ag-AgCl (E^0= -0.047V vs SCE) electrode performed as the reference electrode and glassy carbon electrode (GC) acted as the working electrode [23,24]. The electrode was mechanically refreshed with emery paper of decreased grain size and cleaned with double distilled water. Decimolar solution of tetra butyl ammonium tetra fluoro borate (TBATFB) was employed as the supporting electrolyte. Deaeration was achieved by passing nitrogen gas continuously through the medium. Ivium compactstat-e electrochemical system together with advanced software iviumsoft was used for the computer assisted cyclic voltammetric studies.

Procedure

10^{-3} M solution of the Schiff base or complex was prepared in DMSO and transferred (3ml) into the electrolytic cell, added 2ml of decimolar solution of the supporting electrolyte in DMSO (2ml) and the three electrodes were immersed in the homogeneous mixture. Nitrogen gas was continuously passed through the solution in a controlled manner throughout the experiment. The unstirred solution was scanned for a potential range +2.0V to -2.0V for finding out redox peaks. After detecting the active range of potential in which the compound give well

defined reduction or oxidation peaks, the experiment was repeated with a limited potential range to get more pronounced peaks. Cyclic voltammetric experiments were repeated with another scan rate for validating the nature of redox system (reversible, irreversible or quasi reversible). Scan rates from 20mV/s to 100mV/s were employed for the voltammetric experiments. To verify the adsorption of the compounds on electrode surface, CV studies were performed in 5 cycles at a scan of 100mV/s.

CHAPTER 3

CYCLIC VOLTAMMETRIC STUDIES ON HETEROCYCLIC SCHIFF BASES AND THEIR COMPLEXES

The newly synthesized Schiff base molecules and complexes were subjected to electrochemical investigations using cyclic voltammetry in DMSO medium. Out of the various compounds investigated, only few showed notable response towards the potential scanning. The details are given in the following sections.

Cyclic Voltammetric Studies on 3-Acetylpyridine Semicarbazone

The voltammetric data for 3-acetylpyridine semicarbazone (APSC) is given in Table 4.1. The Schiff base APSC exhibited two well defined cathodic peaks in the forward scan and two anodic peaks in the reverse scan. The cyclic voltammogram of APSC at a scan rate of 20mV/s is depicted in Figure 4.4a. Overlay CV curves at various scan rates (20-80mV) is provided in Figure 4.4b. The CV displayed first reduction peak (E_{pc1}) at -373mV with an associated oxidation peak (E_{pa1}) at -348mV at a scan rate of 20mV/s. The peak separation of this couple was 25mV and increased gradually with increasing the scan rate. This is an evidence for the quasi reversible response of the system. The reduction peak potential (E_{pc1}) was shifted to more negative potential, while the oxidation potential almost remained unaltered with the scan rate. The ratio of anodic current to the cathodic current was less than one; however both i_{pc1} and i_{pa1} increased with the square root of scan rate, suggesting that the electrochemical process is diffusion controlled [25-30]. It is interesting to note that the reduction peak E_{pc1}

was totally disappeared in a 10^{-2}M solution of APSC at a scan rate of 100mV/s. Figure 4.5 shows the variation of peak heights with $\upsilon^{1/2}$.

The second redox couple shown by APSC was at E_{pc2} =276mV and E_{pa2} =425mV. The peak heights were proportional to the square root of the scan rate and can assume that the process is diffusion controlled. The peaks E_{pc2} and E_{pa2} are virtually independent of the scan rate and they behaved more likely as a reversible system, even though the peak ratio i_{pa2}/i_{pc2} was greater than 1 [31-33]. The cathodic peak appeared at 276mV can be regarded due to the reduction of the carbonyl group of the molecule APSC by a one electron transfer process. The main oxidizable moiety present in the molecule is the $–NH_2$ group, which can be characterized by the peak potential appeared at -348 mV at a scan rate of 20mV/s.

Table 4.1 Cyclic voltammetric data of Schiff base APSC

υ (mV/s)	E_{pc1} (mV)	i_{pc1} (µA)	E_{pc2} (mV)	i_{pc2} (µA)	E_{pa1} (mV)	i_{pa1} (µA)	E_{pa2} (mV)	i_{pa2} (µA)	i_{pa2}/i_{pc2}
20	-373	-0.48	276	-0.651	-348	0.793	425	1.12	1.72
40	-403	-0.983	278	-0.873	-336	1.17	425	1.63	1.86
60	-418	-1.09	282	-1.06	-350	1.83	432	2.03	1.91
80	-420	-1.54	279	-1.03	-349	3.14	430	2.45	2.37

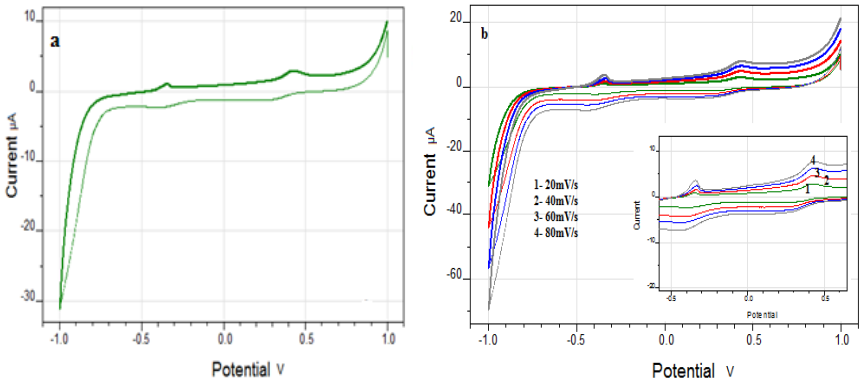

Fig. 4.4 Cyclic voltammogram of APSC a) at scan rate of 20mV/s b) at scan rates 20-80 mV/s

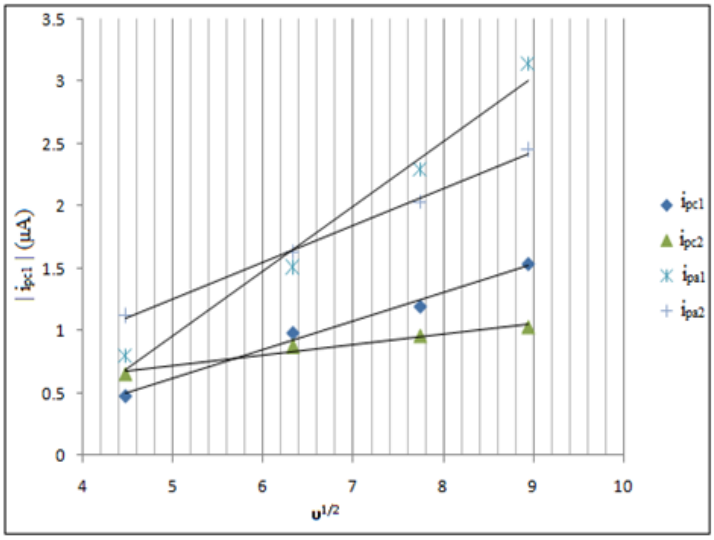

Fig. 4.5 The i_p- $\upsilon^{1/2}$ curves for the Schiff base APSC

To check the adsorption [34-36] of APSC on electrode surface, multi cycle voltammetry was performed at scan rate of 100mV/s. Figure 4.6 shows the consecutive CV diagrams for APSC with 5 cycles vs Ag/Ag+ electrode. Since the peak heights were not reduced appreciably during multiple scanning processes, it is desirable to assume that the Schiff base APSC is not adsorbing appreciably on the glassy carbon electrode surface.

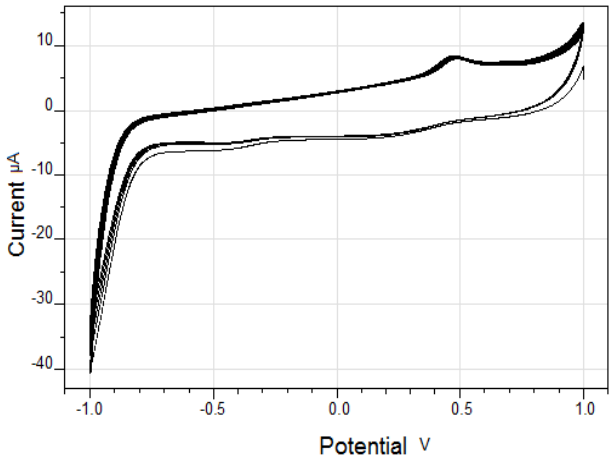

Fig. 4.6 Consecutive CV diagrams for APSC at scan rate of 100mV/s with 5 cycles

Cyclic Voltammetric Studies on VO(II)-APSC Complex

The voltammetric behaviour of VO(II) complex of APSC was characterized by one oxidation peak in DMSO medium at glassy carbon electrode. The oxidation potential was at 421 mV vs Ag/Ag+ at a scan rate of 40mV/s and the peak height corresponds to one electron transfer process. The position of oxidation peak was almost same as one of the oxidation peak displayed (E_{pa2}) by the Schiff base APSC, which attributes that the free groups of the ligand, which are not participating in the complexation process underwent oxidation on the surface of the glassy carbon electrode. During the forward scan, the reduction peak was not appeared in the cyclic voltammogram, but on increasing the sweep rate, appearance of small shoulder at about 125mV was the indication of reduction of VO(II) complex. Since the separation of anodic and cathodic peaks was considerably large (about 320mV) at a scan rate of 100mV/s, it suggests that the redox system behave in a quasi reversible manner. Figure 4.7a and 4.7b show the cyclic voltammograms of VO(II)-APSC complex at the scan rate 40mV/s and at various scan rates (40-100mV/s) respectively. Cyclic voltammetric data of this complex is listed in Table 4.2.

From the data, it is evident that the oxidation peak gradually shifted to more positive potential with the scan rate, suggesting that the electrode process deviate slightly from the reversible character. Figure 4.8 portrays the i_p- $\upsilon^{1/2}$ graph of VO(II)-APSC complex for anodic peak currents (i_{pa}). As seen from the plot, the peak current obtained at different scan rates were observed to change linearly with

the square root of the scan rate, which attributes the diffusion controlled rate determining electrode process.

Table 4.2 Cyclic voltammetric data of VO(II)-APSC complex

υ (mV/s)	E_{pa} (mV)	i_{pa} (µA)	$i_{pa} / \upsilon^{1/2}$
40	421	0.594	0.093
60	427	0.716	0.092
80	432	0.748	0.083
100	444	0.938	0.094

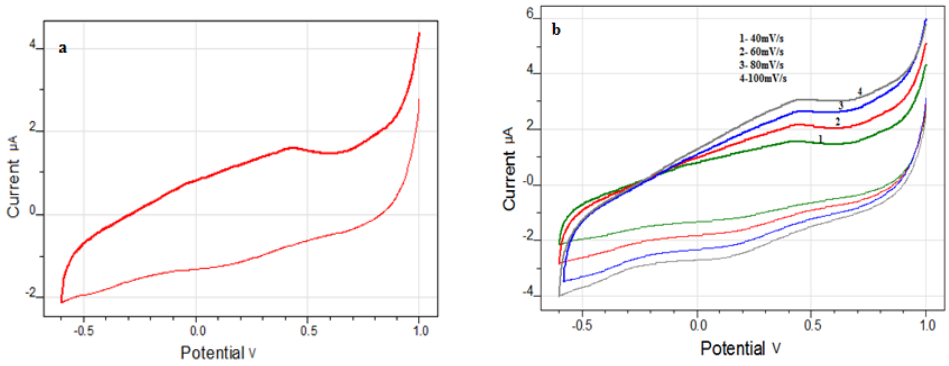

Fig. 4.7 Cyclic voltammogram of VO(II)-APSC complex a) at scan rate of 40mV/s b) at scan rates 40-100 mV/s

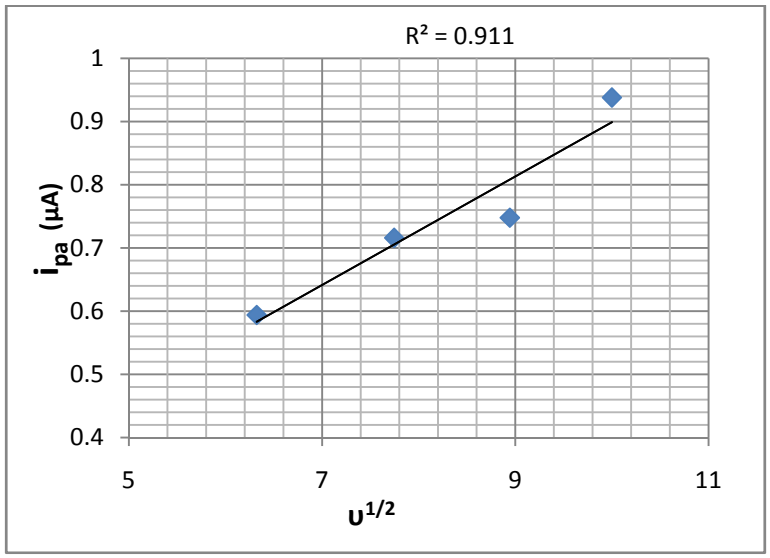

Fig. 4.8 The i_p- $\upsilon^{1/2}$ curves for VO(II)-APSC complex

Cyclic voltammetric Studies on Ni(II)-APSC Complex

The nickel complex of APSC did not exhibit any cathodic peaks in the forward scan, but a well defined oxidation peak was shown in the reverse scan. The absence of any cathodic peak is an indication of the reluctance of Ni(II)-APSC complex to take part in the reduction process, which in turn supports the highly stable nature of the complex. At a scan rate of 40mV/s the oxidation peak was appeared at 215mV for a concentration of 10^{-3}M of the complex in DMSO. Appearance of this peak can be attributed to the oxidation of free ends of the Schiff base, which are not participated in the complex formation (may be $-NH_2$ group). The cyclic voltammetric data of the complex Ni(II)-APSC is provided in Table 4.3. It is understandable from the table that as the scan rate was increased, the peak potential shifted to positive potential, which indicates the irreversible nature of the electrochemical process. Peak current i_{pa} was also increased with the scan rate. The current function $i_{pa}/\upsilon^{1/2}$ has been found to be appreciably constant with respect to the scan rate indicating that the electrode process is diffusion controlled. The cyclic voltammogram of the complex is given in the Figure 4.9 and the variation of the peak height with square root of the scan rate is depicted in Figure 4.10.

Table 4.3 Cyclic voltammetric data of Ni(II)-APSC complex

υ (mV/s)	E_{pa} (mV)	i_{pa} (μA)	$i_{pa} / \upsilon^{1/2}$
40	215	0.294	0.046
60	256	0.383	0.049
80	260	0.432	0.048
100	266	0.501	0.050

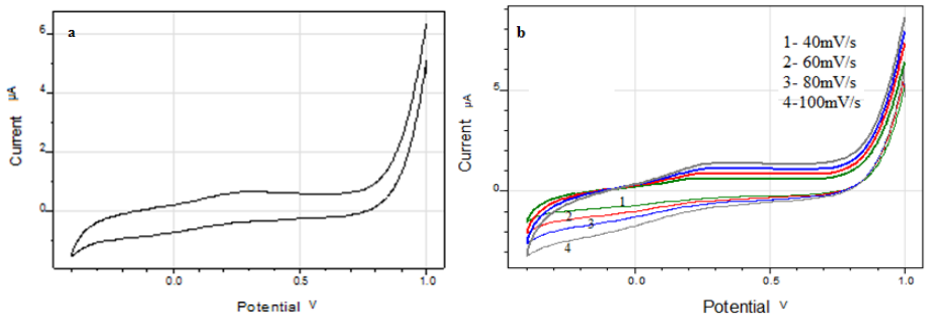

Fig. 4.9 Cyclic voltammogram of Ni(II)-APSC complex a) at scan rate of 40mV/s b) at scan rates 40-100 mV/s

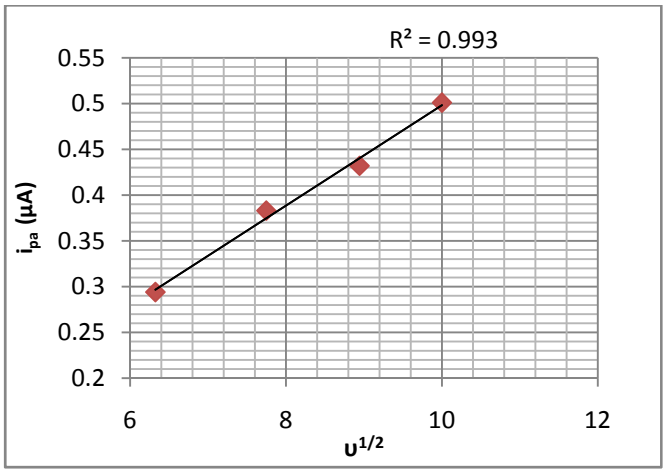

Fig. 4.10 The i_{pa}- $\upsilon^{1/2}$ curves for Ni(II)-APSC complex

Cyclic Voltammetric Studies on Cu(II)-APSC Complex

The cyclic voltammogram of Cu(II)-APSC complex is represented in Figure 4.11. The voltammogram at a scan rate of 20mV/s displayed one well defined reduction peak at -52mV (E_{pc}) associated with an oxidation peak (E_{pa2}) at 500mV (vs Ag/Ag^{+}). The cathodic electrode process was irreversible in nature and the peak potential shifted to more negative potential with increasing scan rate. The quasi reversible nature of the redox couple was established, since peak potential difference (ΔE_p) was about 550mV at lower scan rates. The reduction process can be attributed to the Cu(II)/Cu(I) couple of the metal chelate in DMSO medium. At all scan rates the ratio of anodic to cathodic peak height was greater

than one which supports the quasi reversible nature of the redox system. The oxidation peak was also shifted to more positive side with increasing the sweep rate. For every responses, the cathodic (i_{pc}) and anodic (i_{pa2}) peak heights varied with the square root of sweep rate (Figure 4.12 and 4.13) and can assume that the mass transport in redox process is mainly controlled by the diffusion. Table 4.4 describes the CV data of Cu(II)-APSC complex.

Multicycle CV experiment was performed on Cu(II)-APSC complex at a scan rate of 100mV/s with 5 cycles and the voltammogram is depicted in Figure 4.14. Since the peak heights were not affected seriously with the number of cycles, it can be assumed that the complex is not adsorbed on the electrode surface appreciably by adsorption.

In addition to the redox couple Cu(II)/Cu(I) appeared in the cyclic voltammogram, an oxidation shoulder was appeared at about 64mV (E_{pa1}), which was shifted to more negative potential with the scan rate. It is worthwhile to note that the peak height gradually diminished with the scan rate and totally disappeared in the multi cycle experiment. From the structural elucidation studies of complexes (part I), it was confirmed that the Cu(II) complex of APSC acquired a bridged structure (μ-acetato complex). It may be assumed that the appearance of the small oxidation peak at 64mV at a low scan rate of 20mV/s, is due to the oxidation of the bridging acetate moiety, and this was not taking place at higher scan rates.

From the foregoing discussions the overall reaction describing the electrode reaction of Cu(II)-APSC complex in DMSO can be proposed as in Figure 4.15.

Table 4.4 Cyclic voltammetric data of Cu(II)-APSC complex

υ (mV/s)	E_{pc} (mV)	i_{pc} (μA)	E_{pa1} (mV)	i_{pa1} (μA)	E_{pa2} (mV)	i_{pa2} (μA)	i_{pa2}/i_{pc}
20	-52	-12.0	64	10.9	500	18.7	1.56
40	-108	-14.7	37	5.06	536	22.2	1.51
60	-149	-16.1	28	3.22	546	26.3	1.63
80	-169	-16.9	11	1.81	572	28.2	1.66
100	-189	-17.0	16	1.30	583	30.1	1.77

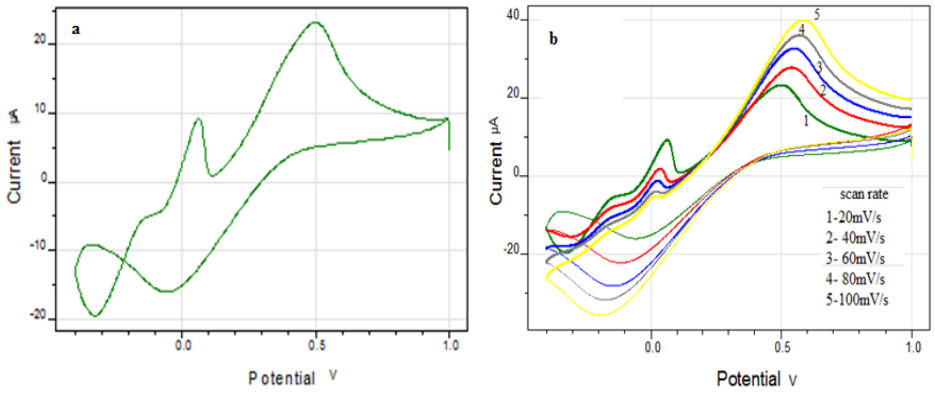

Fig. 4.11 Cyclic voltammogram of Cu(II)-APSC complex a) at scan rate of 20mV/s b) at scan rates 20-100 mV/s

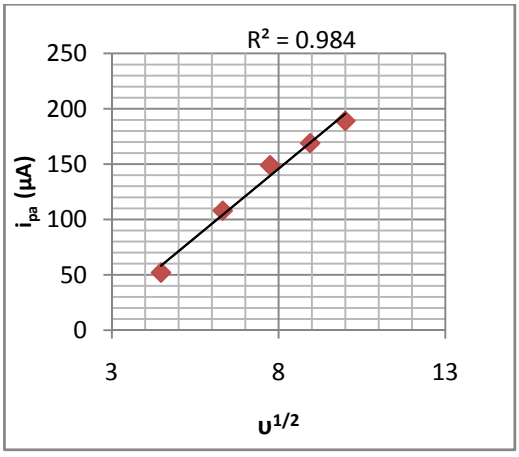

Fig. 4.12 The i_{pc}- $\upsilon^{1/2}$ curves for Cu(II)-APSC complex

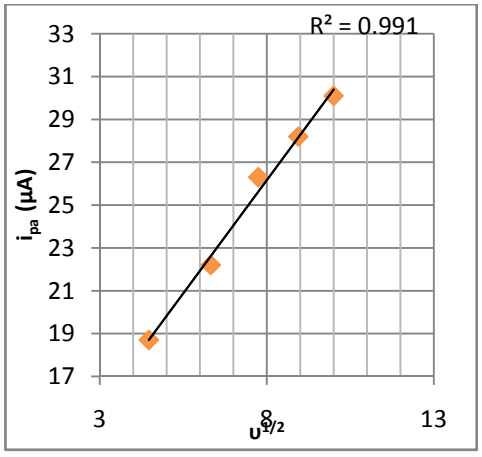

Fig. 4.13 The i_{pa2}- $\upsilon^{1/2}$ curves for Cu(II)-APSC complex

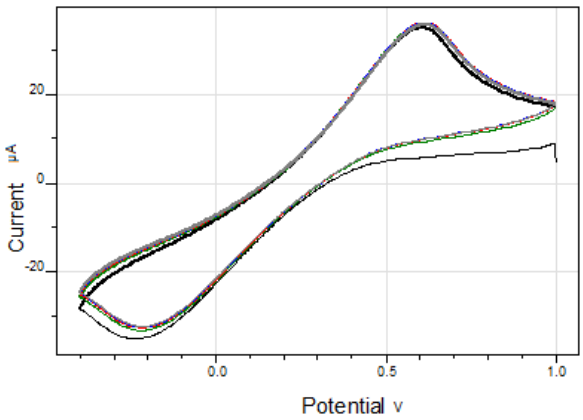

Fig. 4.14 Consecutive CV diagrams for Cu(II)-APSC at scan rate of 100mV/s with 5 cycles

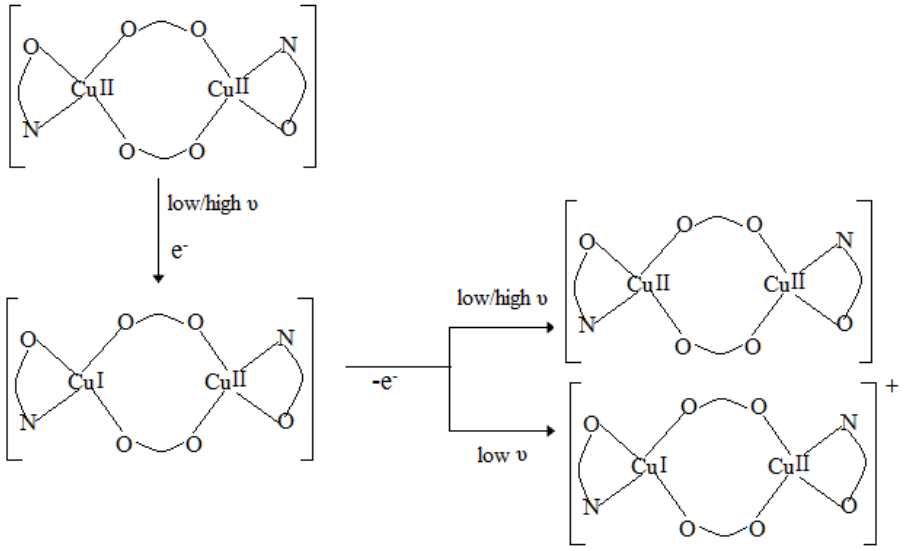

Fig. 4.15 Proposed mechanism for the redox process of Cu(II)-APSC complex

Cyclic Voltammetric Studies on Cd(II)-APSC Complex

Cyclic voltammetric behaviour of Cd(II)APSC complex was evaluated between a potential range of +1000mV to -1500mV at the glassy carbon electrode vs Ag-AgCl refernce electrode. The voltammogram obtained at a scan rate of 40mV/s and the overlay curves for the scan rates 40-100mV are depicted in Figures 4.16 a and 4.16b respectively. The CV diagram of Cd(II) complex

exhibited distinct peaks for oxidation and reduction. The cathodic peak was appaered in the forward scan at -1274mV and the oxidation peak was very clear in the reverse scan, which was appeared at -489mV at a scan rate of 40mV/s. Compared to the CV of the Schiff base APSC, this complex showed different redox behaviour and the peaks were appeared at higher potentials, which indicates that no redox peaks due to the ligand are appearing in the CV of the complex. This suggests a strong complexation between Cd(II) and the Schiff base APSC.

As the sweep rate was increased, the cathodic peak become more negative and the anodic peak moved to positive direction, which confirms the irreversible nature of the electron transfer process. The separation between the cathodic and anodic peaks (ΔE_p) was 785mV at a scan rate of 40mV/s and showed an abrupt rise with scan rate, suggesting the quasi reversible bahaviour of the redox system.

To verify the rate controlling steps of the electrode process, peak heights were plotted against the square root of the sacn rate and found that the cathodic peak current was not proportional to the $\upsilon^{1/2}$, while the anodic peak current maintained proportionality with the square root of scan rate (Figure 4.17), suggesting that the reduction process was more irreversible and charge transfer may be the rate determining process predominantly. Since the anodic peak current was directly proportional to the square root of υ, diffusion is the chief controlling process which governs the rate of electrode reaction. Voltammetric data of cadmium complex is provided in Table 4.5.

Taking into account the voltammetric behaviour of the complex, one can propose the simple mechanism for the electrochemical behaviour of Cd(II)- APSC

complex in DMSO. The cathodic peak can be assigned to the reduction of Cd(II) complex into Cd(I) complex in a quasi reversible mechanism (more close to irreversibility).

$$\text{Cd(II)-APSC complex} + e^- \longrightarrow \text{Cd(I)-APSC complex}$$

The anodic peak appeared in the reverse scan can be considered as the oxidation of Cd(I)-APSC complex into Cd(II)-APSC complex.

$$\text{Cd(I)-APSC complex} \longrightarrow \text{Cd(II)-APSC complex} + e^-$$

It can be determined by cyclic voltammetry whether the complex adsorbed on the electrode surface or not, and it can be verified by multiple cyclic voltammetry. As shown in Figure 4.18, which is the consecutive cyclic voltammograms of Cd(II)-APSC complex with 5 cycles and at 100mV scan rate, the peak height (current) decreased to almost half of that of the first scan, which can be attributed to the appreciable coverage of the electrode surface by Cd(II) complex.

Table 4.5 Cyclic voltammetric data of Cd(II)-APSC complex

υ (mV/s)	E_{pc} (mV)	i_{pc} (μA)	E_{pa} (mV)	i_{pa} (μA)	i_{pa}/i_{pc}	$i_{pc}/\upsilon^{1/2}$	$i_{pa}/\upsilon^{1/2}$	ΔE_p
40	-1274	-57.8	-489	65.9	1.14	9.1	10.4	785
60	-1340	-48.4	-406	84.2	1.73	6.2	10.9	934
80	-1366	-40.5	-202	103	2.54	4.5	11.5	1164
100	-1400	-31.6	-9	115	3.6	3.16	11.5	1391

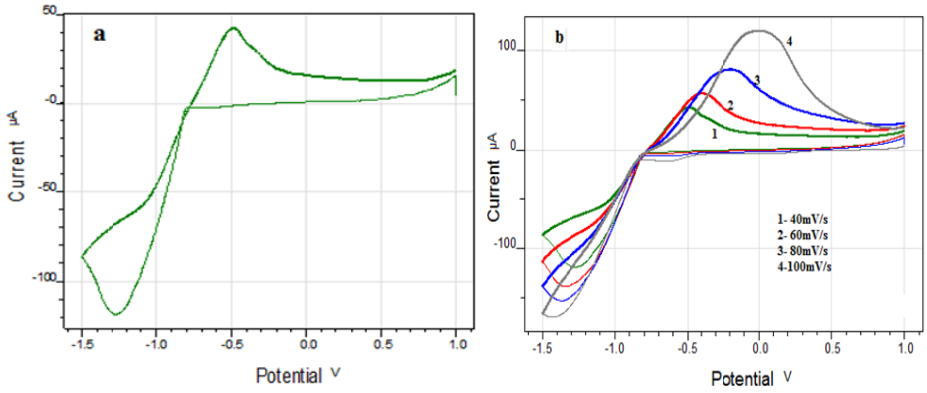

Fig. 4.16 Cyclic voltammogram of Cd(II)-APSC complex a) at scan rate of 40mV/s b) at scan rates 40-100 mV/s

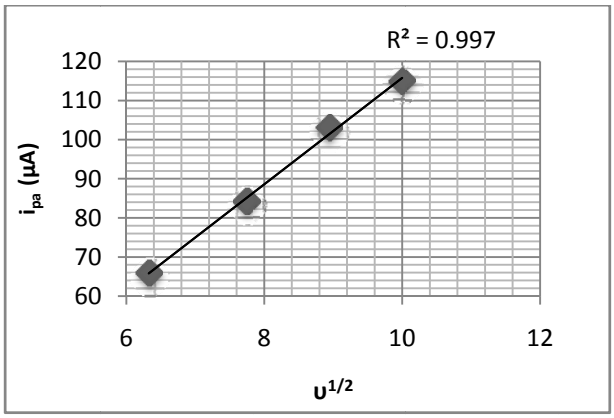

Fig. 4.17 The i_{pa}- $\upsilon^{1/2}$ curves for Cd(II)-APSC complex

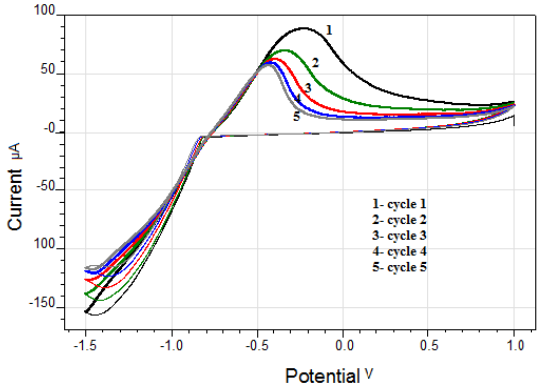

Fig. 4.18 Consecutive CV diagrams for Cd(II)-APSC at scan rate of 100mV/s with 5 cycles

Cyclic Voltammetric Studies on 3-Acetylpyridine Phenylhydrazone

The Schiff base 3-acetylpyridine phenylhydrazone (APPH) was subjected to electrochemical investigations in DMSO medium and reported in this section. The CV diagram of APPH exhibited one reduction and oxidation peak and the redox couple behaved more close to a reversible system. The peak potentials (E_p) were independent of the scan rate, suggesting the behaviour of the reversible system. The peak separation (E_{pa}-E_{pc}) was comparable with the values of reversible redox couples and was independent on the rate of sweep. But the ratio of peak heights was greater than one and showed gradual rise with the scan rate. The cathodic peak current was not strictly proportional to the square root of sweep rate, but the anodic current exhibited fair proportionality to $\upsilon^{1/2}$ (Figure 4.20). Even though, some parameters emphasize the reversibility of the redox process, the actual electrochemical response of this system fall in the quasi reversible spectrum of compounds. Figure 4.19a and 4.19b display the cyclic voltammogram of the Schiff base APPH at scan rate 40mV/s and overlay contours of the voltammograms at various scan rates respectively. The voltammetric data of the compound APPH is provided in Table 4.6.

Table 4.6 Cyclic voltammetric data of Schiff base APPH

υ (mV/s)	E_{pc} (mV)	i_{pc} (μA)	E_{pa} (mV)	i_{pa} (μA)	i_{pa}/i_{pc}	$i_{pc}/\upsilon^{1/2}$	$i_{pa}/\upsilon^{1/2}$	ΔE_p (mV)
40	578	0.62	736	0.96	1.55	0.098	0.15	158
60	580	0.79	740	1.35	1.71	0.10	0.17	160
80	579	0.78	740	1.88	2.41	0.087	0.21	161
100	580	0.75	735	2.28	3.04	0.075	0.22	155

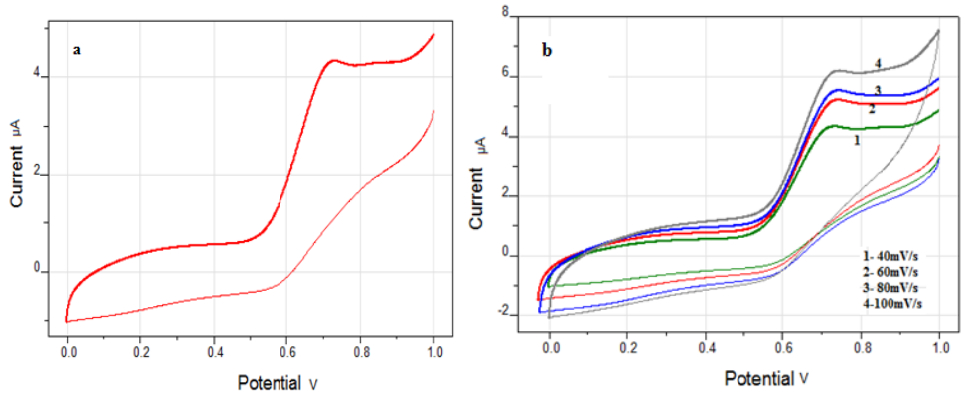

Fig. 4.19 Cyclic voltammogram of APPH a) at scan rate of 40mV/s b) at scan rates 40-100mV/s

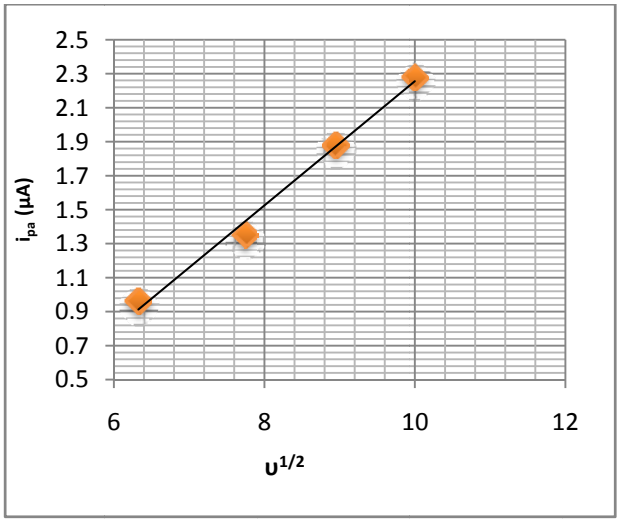

Fig. 4.20 The i_{pa}- $\upsilon^{1/2}$ curves of Schiff base APPH

Cyclic Voltammetric Studies on Cu(II)-APPH Complex

Cyclic voltammogram of Cu(II)-APPH complex at scan rate 20mV/s is provided in Figure 4.21. In the forward scan, the voltammogram had two well defined cathodic waves with first peak (E_{pc1}) situated at more negative cathodic potential and the second peak appeared at a less cathodic potential. As the sweep increased both cathodic peaks were shifted to more negative potentials and at higher scan rates the E_{pc1} peak was disappeared. On reverse scan, two oxidation peaks were exhibited in the cyclic voltammogram, whose potentials are

designated as E_{pa1} and E_{pa2}. On close examination of the voltammogram, it is clear that E_{pa1} and E_{pa2} are the genuine counter peaks of cathodic peaks E_{pc1} and E_{pc2} respectively. Both counter peaks were shifted to more positive potential as the scan rate was increased. The peak separation values of cathodic and anodic peaks suggest that the redox system is behaving as quasi reversible. Cyclic voltammetric data of Cu(II)-APPH complex is given in Table 4.7.

Table 4.7 Cyclic voltammetric data of Cu(II)-APPH complex

υ (mV/s)	E_{pc1} (mV)	i_{pc1} (µA)	E_{pc2} (mV)	i_{pc2} (µA)	E_{pa1} (mV)	i_{pa1} (µA)	E_{pa2} (mV)	i_{pa2} (µA)	i_{pa1}/i_{pc1}	i_{pa2}/i_{pc2}	ΔE_{p1}	ΔE_{p1}
20	-737	-2.0	-197	-0.58	-58	2.79	577	0.64	1.4	1.1	679	774
40	-810	2.24	-227	-0.91	-43	4.07	599	0.81	1.8	0.94	767	826
60	-876	1.95	-263	-0.78	-29	4.92	606	0.89	2.5	1.14	847	869
80	-	-	-591	0.367	-14	5.08	628	0.91	-	2.4	-	1219

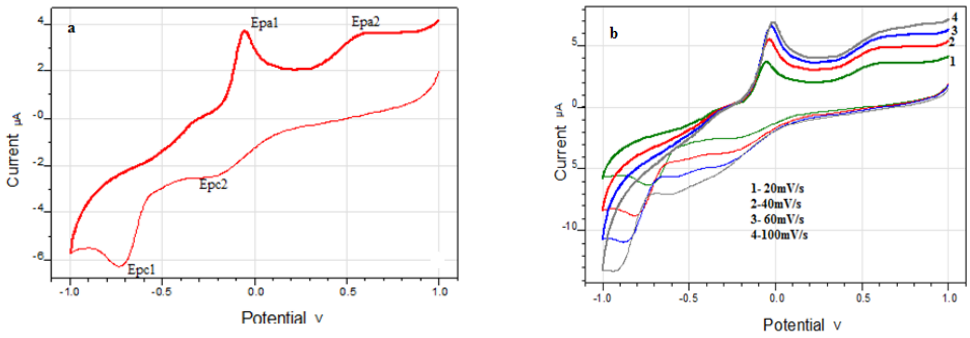

Fig. 4.21 Cyclic voltammogram of Cu(II)-APPH complex a) at scan rate of 20mV/s b) at scan rates 20-80mV/s

Taking into consideration the cyclic voltammetric response of Cu(II)-APPH complex, one can propose the mechanism of electrochemical reactions as follows.

The first cathodic curve can be assigned to the cathodic reduction of Cu(II)-complex to the Cu(I)-complex in a quasi reversible mechanism, since there is a negative shift to cathodic peak potential with increase in the scan rate (however, i_{pc1} was not proportional to the square root of scan rate).

$Cu(II)\text{-complex} + e^- \rightarrow Cu(I)\text{-complex}$

The second cathodic peak, which arise in the more negative potential to that of the first reduction peak is assignable to the reduction of Cu(I)-complex to the Cu(0)-complex. Since the E_{pc2} was also moved to the higher negative potentials with the scan rate, quasi reversible nature of the electrode process can be assumed. The peak height was not proportional to the square root of scan rate.

$Cu(I)\text{-complex} + e^- \rightarrow Cu(0)\text{-complex}$

The stability of Cu(0) -complex is very low and the ligand molecules may or may not detach (decomplexation) from the metal atom within a short span. So the concentration of Cu(0)-complex in the immediate vicinity of the carbon electrode will be very low. The first anodic peak appeared, which was the counter peak of E_{pc1}, is due to the anodic oxidation of Cu(0)-complex.

$Cu(0)\text{-complex} \rightarrow Cu(I)\text{-complex} + e^-$

The height of this anodic peak was high and showed proportionality with $\upsilon^{1/2}$ (Figure 4.22) which may be due to the combined oxidation of unstable Cu(0)-complex and free Cu atoms adjacent to the electrode. The second anodic peak appeared at high positive potential can be assigned to the anodic oxidation of Cu(I)-complex to Cu(II)-complex in a quasi reversible manner. This peak was shifted to more positive potentials with the scan rate and the anodic current was proportional to $\upsilon^{1/2}$ (Figure 4.23).

$Cu(I)\text{-complex} \rightarrow Cu(II)\text{-complex} + e^-$

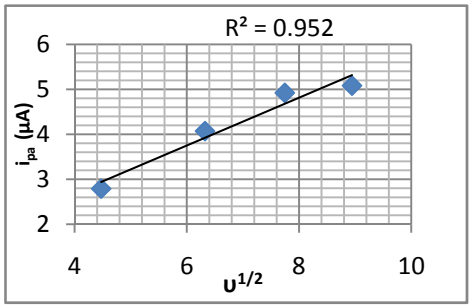

Fig. 4.22 The i_{pa1}- $\upsilon^{1/2}$ curves of Cu(II)- APPH complex

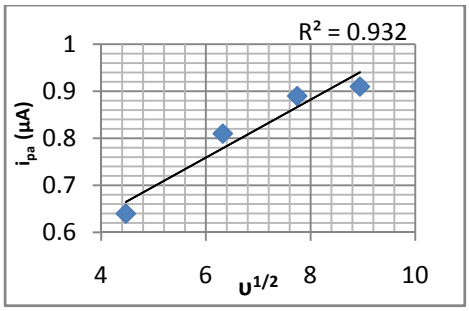

Fig. 4.23 The i_{pa2}- $\upsilon^{1/2}$ curves of Cu(II)- APPH complex

Cyclic Voltammetric Studies on Furan-2-Aldehyde-3-Aminobenzoic Acid

The Schiff base furan-2-aldehyde-3-aminobenzoic acid (FAABA) copper gave appreciable response towards electrochemical investigation. The Schiff base displayed one cathodic reduction peak at 94V at scan rate of 40mV/s in the cyclic voltammogram and the peak was shifted to more cathodic side with increase in the sweep rate. The cathodic peak appeared in this region can be assigned to the reduction of the azomethine moiety of the Schiff base. On the reverse scanning process, a more prominent anodic wave was appeared at about 390mV which might not have appeared by the oxidation of the already reduced species, since the peak separation difference was very high (>290mV). The anodic electrode process was not altered significantly with the scan rate, since the peak position was appeared in the same oxidation potential and the peak height was proportional to the scan rate. As a whole, the redox behaviour of the Schiff base (FAABA) is more equivalent to an irreversible system. The cyclic voltammogram and the voltammetric data of the Schiff base FAABA is given in Figure 4.24 and Table 4.8 respectively.

Table 4.8 Cyclic voltammetric data of the Schiff base FAABA

υ (mV/s)	E_{pc} (mV)	i_{pc} (μA)	E_{pa} (mV)	i_{pa} (μA)	i_{pa}/i_{pc}	ΔE_p	$i_{pc}/\upsilon^{1/2}$	$i_{pa}/\upsilon^{1/2}$
40	94	-0.20	384	0.53	2.65	290	0.031	0.084
60	91	-0.22	381	0.61	3.05	290	0.026	0.079
80	44	-0.25	390	0.69	2.76	346	0.028	0.077
100	33	-0.38	390	0.91	-2.39	357	0.038	0.091

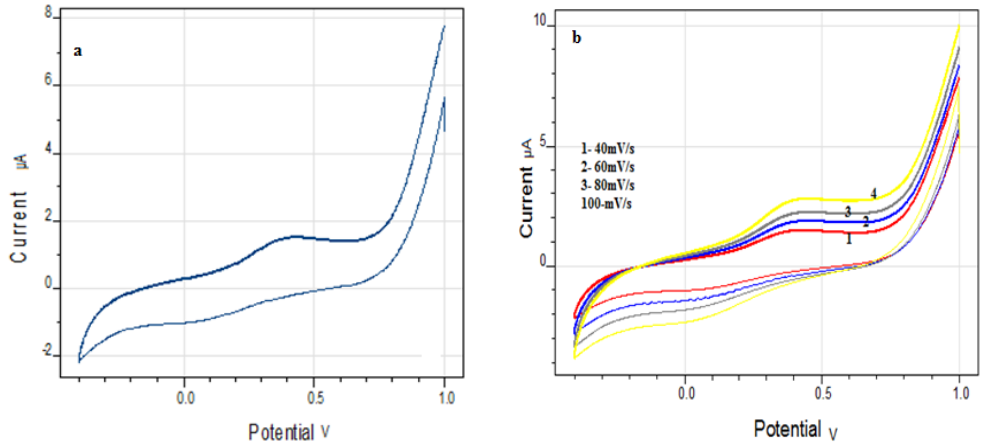

Fig. 4.24 Cyclic voltammogram of FAABA a) at scan rate of 40mV/s b) at scan rates 40-100mV/s

The anodic and cathodic peak currents were proportional to $\upsilon^{1/2}$ at lower scan rates indicating that both processes are diffusion controlled rather than pure charge transfer controlled at lower scan rates, but deviation from the proportionality was noted for both anodic and cathodic peak heights at higher scan rate (Figure 4.25).

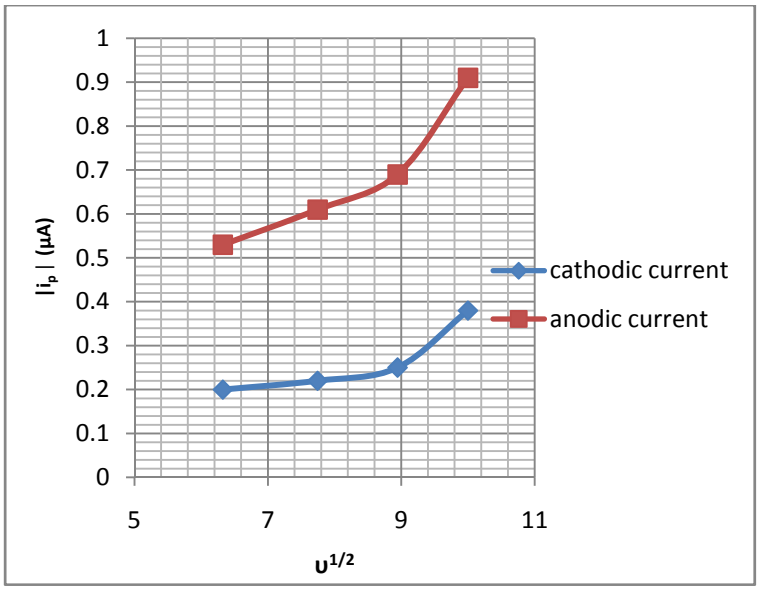

Fig. 4.25 The i_p- $\upsilon^{1/2}$ curves of Schiff base FAABA

Cyclic Voltammetric Studies on Cu(II)-FAABA Complex

The cyclic voltammogram of 10^{-3}M Cu(II)-FAABA complex in DMSO at scan rate 20mV/s is provided in Figure 4.26. The voltammogram displays one broad cathodic reduction peak and two anodic oxidation peaks. The second anodic peak (E_{pa2}) was very prominent and appeared at high positive potential. The cathodic peak was shifted to more negative potentials with the sweep rate, moreover i_{pc} was proportional to $\upsilon^{1/2}$ (Figure 4.27), indicate the diffusion controlled process. The cathodic curve and the first anodic shoulder (E_{pa1}) is assignable to the Cu(II)/Cu(I) redox couple, responding in a quasi reversible manner. The peak separation of these redox couple was decreased with the scan rate. Table 4.9 shows the voltammetric data of the Cu(II)-complex of FAABA. Though it is very difficult to determine a precise mechanism of the electrochemical behaviour of this redox system, the second oxidation peak which appeared at a higher potential than the former one can be attributed to the

oxidation of Cu(II)-complex into Cu(III)-complex. During this electrode reaction, the peak current was not followed proportionality with the square root of the scan rate. The overall mechanism for the electrochemical response of Cu(II)-FAABA complex can be proposed as follows:

$[Cu(II)L] + e^- \rightarrow [Cu(I)L]$

$[Cu(I)L] \rightarrow [Cu(II)L] + e^-$

$[Cu(II)L] \rightarrow [Cu(III)L] + e^-$

To check the extent of adsorption of the complex on the glassy carbon electrode surface, multi cycle cyclic voltammetry was performed (Figure 4.28). Since considerable lowering of the cathodic peak height was noted for the last cycle CV wave on comparison with the first cycle CV wave, one can imagine that appreciable adsorption of the complex was took place during the electrode reactions.

Table 4.9 Cyclic voltammetric data of Cu(II)-FAABA complex

υ (mV/s)	E_{pc} (mV)	i_{pc} (μA)	E_{pa1} (mV)	i_{pa1} (μA)	E_{pa2} (mV)	i_{pa2} (μA)	i_{pa1}/i_{pc1}	ΔE_{p1}	$i_{pc}/\upsilon^{1/2}$
20	70	-0.42	-175	0.166	770	2.39	0.39	245	0.093
40	-106	-0.50	-156	0.19	840	2.47	0.38	50	0.079
60	-161	-0.61	-154	0.22	830	2.27	0.4	7	0.071
80	-157	-0.71	-141	0.20	830	1.97	0.28	16	0.079
100	-182	-0.77	-140	0.24	828	1.99	0.31	42	0.077

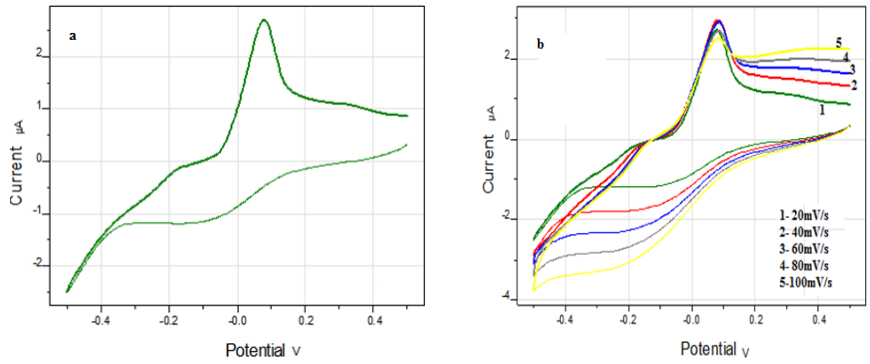

Fig. 4.26 Cyclic voltammogram of Cu(II)-FAABA complex a) at scan rate of 20mV/s b) at scan rates 20-100mV/s

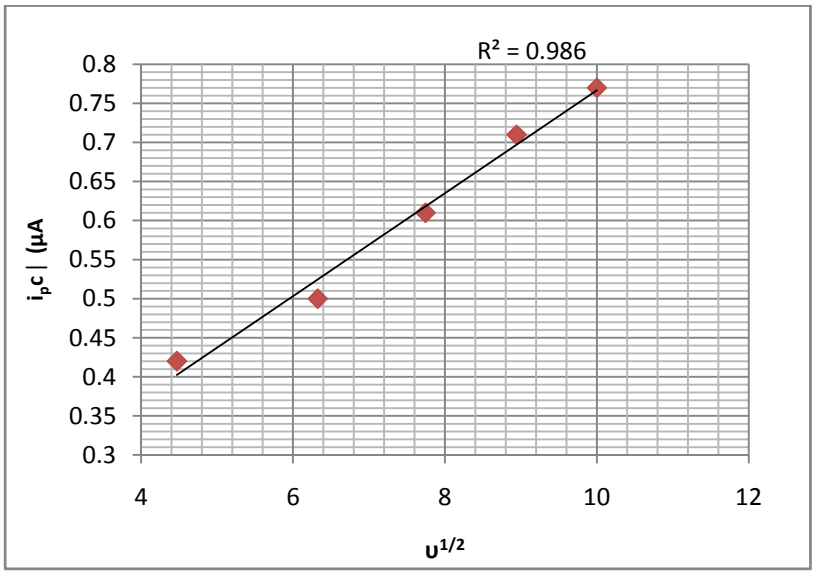

Fig. 4.27 The i_{pc}- $\upsilon^{1/2}$ curves for Cu(II)-FAABA complex

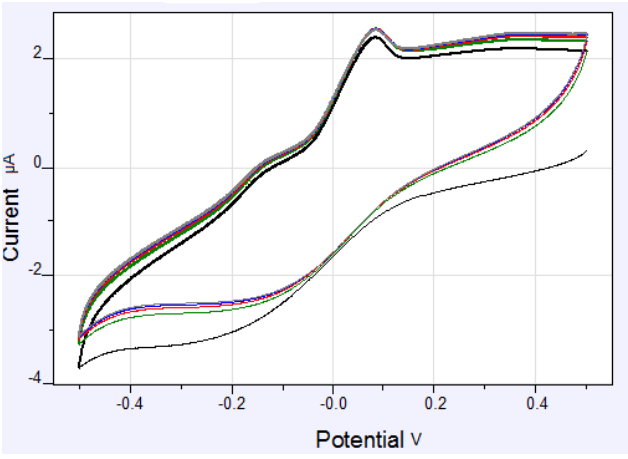

Fig. 4.28 Consecutive CV diagrams for Cu(II)-FAABA complex at scan rate of 100mV/s with 5 cycles

Cyclic Voltammetric Studies on 3-Acetylpyridine Thiosemicarbazone and its Cu(II) Complex

3-acetylpyridine thiosemicarbazone (APTSC) and its copper complex were subjected to electrochemical studies in DMSO medium and the results are compared and discussed in the subsequent paragraphs. Figure 4.29 displays the voltammogram of APTSC in DMSO at a scan rate of 40mV/s. The CV diagram consist of only one reduction peak appeared at -736mV and the peak potential was found to be shifted to more negative potential with the scan rate, suggesting that the electrode reaction was not reversible.

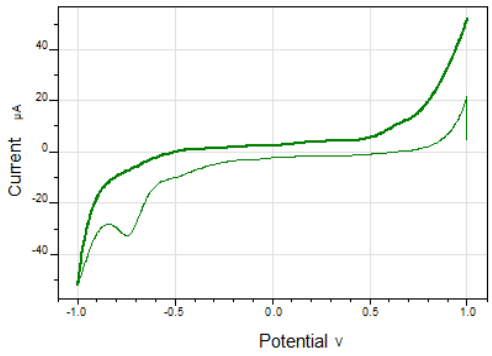

Fig. 4.29 Cyclic voltammogram of APTSC at scan rate of 40mV/s

The copper complex of APTSC exhibited two well defined cathodic waves on the forward scan with first cathodic peak (E_{pc1}) situated at less negative potential and a second cathodic peak (E_{pc2}) appeared at more negative potentials. As the sweep rate was increased, both cathodic waves shifted to more negative potentials. Figure 4.30 shows the cyclic voltammogram of Cu(II)-APTSC complex in DMSO at the scan rate 40mV/s. The cathodic peaks E_{pc1} and E_{pc2} respectively appeared at -314 and -672mV. On reverse scan, an anodic peak was appeared, which was the genuine counter peak of the first cathodic peak (E_{pc1}).

This anodic counter peak was shifted to more positive potential with the scan rate and the peak height was proportional to $\upsilon^{1/2}$ (Figure 4.31). The CV data of Cu(II)-APTSC complex is provided in Table 4.10.

The first cathodic wave appeared at -314mV and the anodic peak were assignable to the redox couple Cu(II)/Cu(I). The ratio of peak current to the square root of the scan rate was not constant for the two cathodic waves, suggesting the quasi reversible nature of the electrode process. On comparing the voltammogram of the ligand and complex one can reach into the possible conclusion that the second cathodic wave appeared at -672mV in the CV of the complex is due to the cathodic wave corresponds to the reduction of the ligand APTSC. The response of this cathodic wave (E_{pc2}) was very similar to that of the free ligand, in the sense that the peak potential was moved to more negative potential and the peak height was not directly proportional to the $\upsilon^{1/2}$. After one step reduction of the complex ($Cu^{II} \rightarrow Cu^{I}$), the ligand become partially free, because the valency, electronic arrangement and the geometry of the central metal ion changes significantly, which will favour the easy reduction of the susceptible sites of the ligand (most probably the C=S group). The very prominent anodic peak (which was the counter peak of the first cathodic peak), whose height was comparable to the two electron process, is probably not only due to the conversion of Cu(I)-complex to Cu(II)-complex, but also to the oxidation of the reduced moieties of the organic part. The probable mechanism which explain the redox behaviour of Cu(II) complex of APTSC is depicted in Figure 4.31. The multi cycle voltammogram of the copper complex is shown in Figure 4.32. Peak heights

of the voltammogram establish that electrode surface was less covered by the analyte at scan rate 100mV/s. Second cathodic peak (E_{pc2}) was totally disappeared from the voltammogram on the repeated scanning process.

Table 4.10 Cyclic voltammetric data of Cu(II)-APTSC complex

υ (mV/s)	E_{pc1} (mV)	i_{pc1} (μA)	E_{pc2} (mV)	i_{pc2} (μA)	E_{pa} (mV)	i_{pa} (μA)	i_{pa}/i_{pc1}	$i_{pa}/ \upsilon^{1/2}$	ΔE_p
40	-314	-38	-672	-10.3	792	82.7	2.17	13.07	1106
60	-380	-37.5	-723	-12.3	847	122.4	3.26	15.80	1227
80	-394	-36.8	-774	-10.7	1000	145.0	3.94	16.21	1394

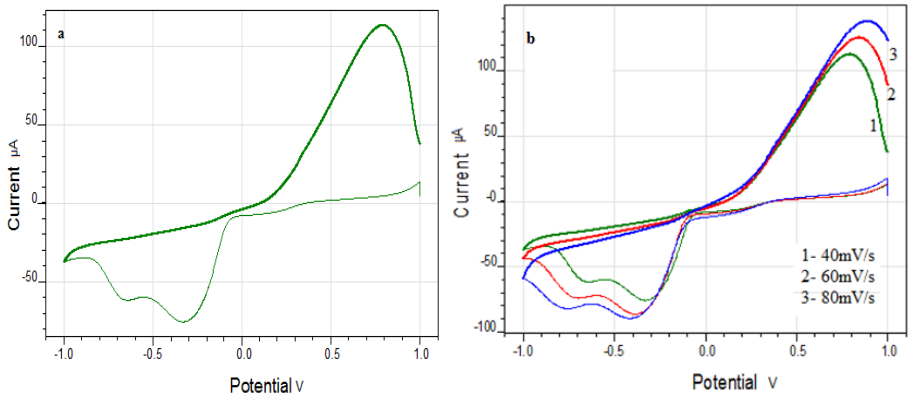

Fig. 4.30 Cyclic voltammogram of Cu(II)-APTSC complex a) at scan rate of 40mV/s b) at scan rates 40-80mV/s

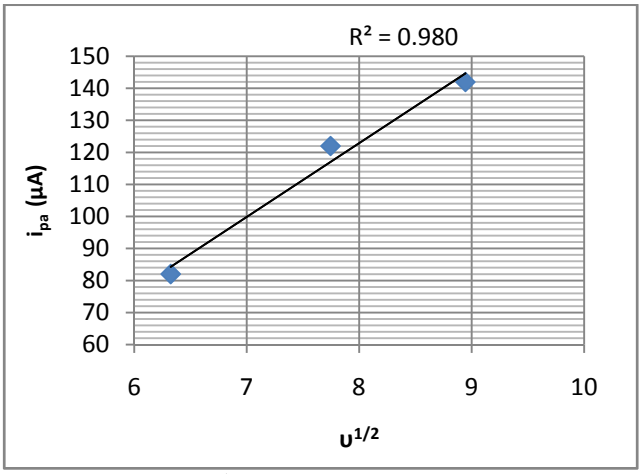

Fig. 4.31 The i_{pa}- $\upsilon^{1/2}$ curves for Cu(II)-APTSC complex

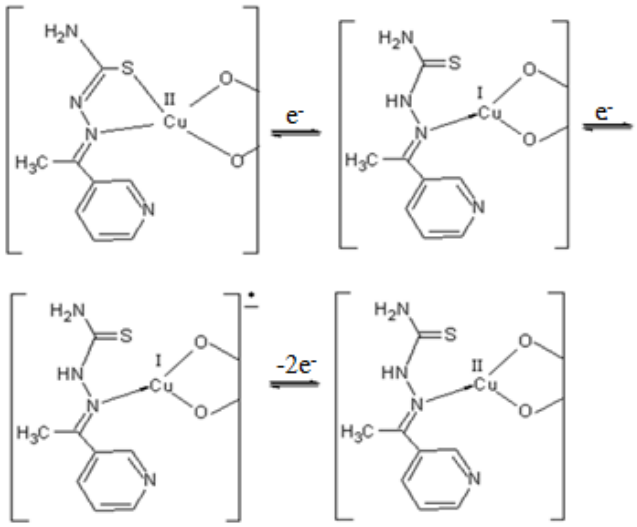

Fig. 4.32 Proposed mechanism for the redox process of Cu(II)-APTSC complex

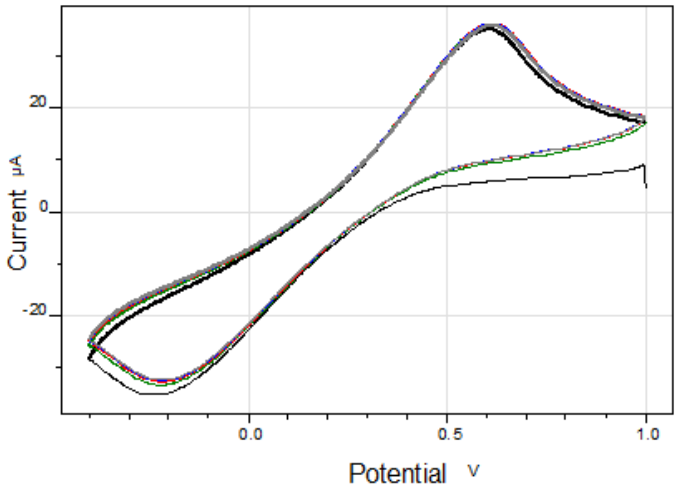

Fig. 4.33 Consecutive CV diagrams for Cu(II)-APTSC at scan rate of 100mV/s with 5 cycles (vs Ag-AgCl electrode)

SUMMARY

To study the electrochemical behaviour of newly synthesized heterocyclic Schiff bases and their transition metal complexes, they were subjected to cyclic voltammetric measurements in DMSO medium at a concentration of 10^{-3}M. Glassy carbon electrode and platinum wire were used as the working and inert electrode respectively for performing CV analysis and Ag-AgCl electrode acted as the reference electrode. The quiescent solutions were scanned for a potential range +200mV to -200mV for finding out redox peaks and the whole experiment was done with the help of Ivium compactstat-e electrochemical system. Out of the various compounds analyzed, only few gave significant response for electrochemical investigation.

The Schiff base, 3-acetylpyridine semicarbazone (APSC) exhibited two cathodic and anodic peaks. Two redox couples were assigned from the cyclic voltammogram and they were identified as quasi reversible redox couples. Vanadyl complex of APSC displayed one redox couple in the cyclic voltammogram with a separation of 320mV, which behaved as a quasi reversible redox system. The anodic peak current was found to increase with the square root of the scan rate and the current function was remained as a constant. Since no cathodic peaks were appeared in the forward scan, the Ni(II)-APSC complex can be assumed to behave as an irreversible system.

One cathodic peak and three anodic peaks were appeared in the cyclic voltammogram of Cu(II)-APSC complex at a low scan rate. The probable mechanism for the electrochemical response was explained by assuming that one

of the metal sites of the bridged chelate undergoes redox process. The appearance of a medium intense anodic peak at low scan rate can be attributed to the oxidation of ligand moieties. The cadmium complex displayed distinct peaks for oxidation and reduction. The separation between the anodic and cathodic peaks was 785mV and showed an abrupt rise with the scan rate, indicating the quasi reversible nature of the system. The mechanism of the electrode reaction is believed to be Cd(II)/Cd(I) redox process. Multicycle CV studies of this complex revealed that considerable adsorption of this compound take place on the electrode surface.

The CV diagram of 3-acetylpyridine phenylhydrazone (APPH) exhibited one redox couple, which behaved more close to a reversible system. The peak potentials were independent of the scan rate and the peak separation was comparable with the values of reversible redox couples and was independent on the rate of sweep. Two well defined cathodic and anodic peaks were noted in the voltammogram of Cu(II)-APPH complex, which was assigned to the Cu(II)/Cu(I) and Cu(I)/Cu(0) redox couples.

Furan-2-aldehyde-3-aminobenzoic acid (FAABA) also showed clear response to CV studies. One cathodic and anodic peaks were visible in the voltammogram of FAABA and the response was more likely to an irreversible system. The cyclic voltammogram of Cu(II)-FAABA insists the conversion of Cu(II)-complex into Cu(III)-complex.

One distinct cathodic peak was clearly visible in the CV diagram of the Schiff base 3-acetylpyridine thiosemicarbazone (APTSC) at -736mV. The Cu(II)-

APTSC complex showed two prominent cathodic peaks and the anodic peak was emerged on the reverse scan process. The appearance of the second cathodic peak may be regarded to the ligand centred reduction process. A probable mechanism for the electrochemical behaviour of this complex is also discussed.

REFERENCES

1. D. H. Evans, K. M. O. Konnell, R. A. Petersen, M. J. Kelly, *J. Chem. Edn.*, 60, 4 (1983) 290.
2. H. Jurgen, *"Cyclic Voltammetry -Electrochemical Spectroscopy"- New Analytical Methods*, 23, 11 (1984) 831
3. B Alan, F. Stephen, *J. Phys. Chem.,* 102 (1998) 9966
4. A. Sevcik, *Chem. Commun.*, 13 (1948) 349
5. J.E.B. Randles, *Trans. Faraday Soc.*, 44 (1948) 327
6. H. Matsuda, Y. Ayabe, *Z. Electrochem.*, 59 (1955) 494
7. R. S. Nicholson, I. Shain, *Anal. Chem.,* 36 (4) (1964) 706
8. C. Gabino, *J. Chem. Educ.,* 65 (1988) 110
9. S. Bankim, S. Ashwini, *Electrochim. Acta,* 55 (2010) 8638
10. A. Perez-Rebolledo, O. E. Piro, E. E. Castellano, L. R. Teixeira, A. A. Batista, H. J. Beraldo, *Mol. Struct.*, 18 (2006) 794
11. W. U. Malik, P. N. Dua, *Indian J. Chem.*, 21A (1982) 1083
12. R. N. Goyal, A. J. Minocha, *J. Indian. Chem. Soc.*, 62 (1985) 202
13. B. B. Reddy, N. Y. Sreedhar, S. J. Reddy, *Indian. J. Chem.*, 30A (1991) 119
14. P. Sharma, A. Kumar, M. Sharma, *Indian J. Chem.*, 45A (2006) 872
15. B. S. Parajon- Costa, A. C. Gonzalez Baro, E. J. Baran, *Z. Anorg. Allg. Chem*., 628 (2002) 1419
16. B. Lotfi1, B. Mustafa, B. Leila, M. Salima, *Int. J. Electrochem. Sci.*, 6 (2011) 1991

17. R. Sangtyani, V. Kumar, R. C. Meena, A. K. Varshney, S. Varshney, *Int. J. Chem. Tech. Res*., 4(1) (2012) 180

18. B. S. C. Oliveiraa, I. P. G. Fernandes, B. V. Silva, A. C. Pinto, A. M. O. Brett, *J. Electroanal. Chem.*, 689 (2013) 207

19. C. R. Kowol, E. Reisener, I. Chiorescu, V. B. Arion, M. Galanski, D. V. Deubel, B. K. Keppler, *Inorg. Chem.*, 47 (23) (2008) 11032

20. B. Sarma, D. Kumar Das, *J. Chem.,* 2013 (2013) ID 349580

21. S. Datta, D. K. Seth, S. Halder, W. S. Sheldrick, H. M. Figge, M. G. B. Drew, S. Bhattacharya, *RSC Adv*., 2 (2012) 5254

22. R. Prabhakaran, R. Huang, S. V. Renukadevi, R. Karvembu, M. Zeller, K. Natarajan, *Inorganica Chim. Acta*, 361 (2008) 2547

23. R. Andruzzi, M. E. Cardinali, A. Trazza, *Electrochim. Acta* 17 (1972) 1524

24. A. K. Gupta, R.S. Sindal, *J. Chem. Sci.*, 121 (2009) 347

25. A. J. Bard, L. R. Faulkner, *"Electrochemical Methods, Fundamentals and Applications"* ,Wiley, New York (1980)

26. M. Noel, K. I. Vasu, *"Cyclic Voltammetry and the Frontiers of Electrochemistry",* Oxford and IBH Publishing Co. Pvt. Ltd, New Delhi (1990)

27. R. S. Nicholson, I. Shain, *Anal. Chem.*, 36 (1994) 722

28. R. N. Adam, "*Electrochemistry at Solid Electrodes*", Marcel Dekker, New York (1996)

29. P. Sharma, A. Kumar, S. Sharma, *Indian J. Chem.*, 43B (2004) 2431

30. P. Sharma, A. Kumar, M. Sharma, S. Upadhyay, *Indian J. Chem.*, 43B (2004) 2653

31. A. M. O. Brett, "*Electrochemistry- Principles, Methods and Applications",* Oxford University Press: Oxford (1996)

32. J. Bard, L. R. Faulkner, "*Electrochemical Methods"*, 2nd edn, John Wiley & Sons, New York (2001)

33. J. D. Mozo, J. Carbajo, J. C. Sturm, L. J. Nuñez-Vergara, R. Moscoso, J. A. Squella, *Anal. Chim. Acta,* 699 *(*2011) 33

34. E. Gökmeşe, *Int. J. Electrochem. Sci.,* 6 (2011) 103

35. P. T. Kissinger, W. R. Heineman, *J. Chem. Educ.*, *60* (9) (1983) 702

36. F. Gökmeşe, E. Gökmeşe, A.O. Solak, M. Işıklan, Z. Kılıç, *J. Electroanal. Chem*., 581 (2005) 46.